

Broadband Homonuclear Decoupling

Mai Van Do * Navin Khaneja †‡

November 10, 2018

Abstract

We present a solution to the problem of decoupling of a homonuclear two-spin system having weak isotropic scalar coupling. We describe non-selective pulse sequences that create an effective field perpendicular to the coupling interaction over a broad range of chemical shifts, with a magnitude proportional to the chemical shifts. Effective decoupling is achieved when the difference in chemical shifts imprinted on the perpendicular field is sufficiently larger than the coupling between the spins. The proposed methods scale down the chemical shifts. The pulse sequences may be useful in various applications in nuclear magnetic resonance spectroscopy.

1 Introduction

In this paper, we study a classical problem in NMR spectroscopy, the problem of Homonuclear Decoupling. The presence of coupling between nuclear spins alters net magnetic field seen by elements of a spin pair. In addition to applied magnetic field the spins also see a small field arising due to the magnetic moment of their

*School of Engineering and Applied Sciences, Harvard University, Cambridge, MA 02138.

†To whom correspondence may be addressed. Email:navinkhaneja@gmail.com

‡Department of Electrical Engineering, IIT Bombay, Powai - 400076, India.

partners. This field arising due to coupling can be oriented along or against the static field depending on the spin orientation of the magnetic moment. As a result a spin precession frequency of spin I is altered to $\nu_I + \frac{J}{2}$ and $\nu_I - \frac{J}{2}$ depending on the orientation of the magnetic moment. This is called splitting of resonance peaks arising due to couplings. These spin multiplets reduce the signal to noise ratio in NMR experiments and complicate interpretation of the spectrum. It is desirable to find methods by which couplings between spins can be decoupled and we can observe just the precession of spins in external magnetic field without being effected by couplings. In this paper, we develop methods to do this spin decoupling using radio frequency irradiation on the spin systems.

2 Ising Couplings

To begin with, we consider two homonuclear spins I and S coupled by an Ising coupling. The Hamiltonian of the system takes the form

$$H = \omega_I I_z + \omega_S S_z + 2\pi J I_z S_z \quad (1)$$

where ω_I and ω_S are chemical shifts of spin I and S and J is the coupling between the spins. We assume $|\omega_I - \omega_S| \gg J$, so called weakly coupled spin system, as a typical case. Our goal is to decouple the spins without precise information of ω_I and ω_S and J and yet observe and measure the chemical shifts.

We accomplish this by a four stage pulse sequence that evolves the following set of Hamiltonians

$$H_1 = \omega_I I_z + \omega_S S_z + 2\pi J I_z S_z + AF_x \quad (2)$$

$$H_2 = -\omega_I I_z - \omega_S S_z + 2\pi J I_z S_z + AF_x \quad (3)$$

$$H_3 = -\omega_I I_z - \omega_S S_z + 2\pi J I_z S_z - AF_x \quad (4)$$

$$H_4 = \omega_I I_z + \omega_S S_z + 2\pi J I_z S_z - AF_x \quad (5)$$

We produce the evolution

$$U = \exp(-iH_4\Delta) \exp(-iH_3\Delta) \exp(-iH_2\Delta) \exp(-iH_1\Delta) \quad (6)$$

To understand the effect of this pulse sequence we proceed in the frame of the toggling chemical shift. In this frame the rf-Hamiltonian transforms to

$$AI_x \rightarrow A(I_x \cos \omega_I t - I_y \sin \omega_I t) \quad (7)$$

$$AI_x \rightarrow A(I_x \cos \omega_I(\Delta - t) - I_y \sin \omega_I(\Delta - t)) \quad (8)$$

$$AI_x \rightarrow -A(I_x \cos \omega_I t + I_y \sin \omega_I t) \quad (9)$$

$$AI_x \rightarrow -A(I_x \cos \omega_I(\Delta - t) + I_y \sin \omega_I(\Delta - t)) \quad (10)$$

For $\omega_I\Delta < 1$, we can expand $\sin \omega_I t \sim \omega_I t$. Adding the four evolutions we find everything adds along y direction and we get

$$\begin{aligned} & \int_0^\Delta A(I_x \cos \omega_I t - I_y \sin \omega_I t) dt + \int_0^\Delta A(I_x \cos \omega_I(\Delta - t) - I_y \sin \omega_I(\Delta - t)) \\ & - \int_0^\Delta A(I_x \cos \omega_I t + I_y \sin \omega_I t) - \int_0^\Delta A(I_x \cos \omega_I(\Delta - t) + I_y \sin \omega_I(\Delta - t)) \\ & = -2A\Delta\omega_I I_y = -4\frac{\theta}{2}\omega_I I_y \end{aligned}$$

where $\theta = A\Delta$. Therefore in the toggling frame of the chemical shifts, to first order, the net evolution we produce an effective evolution

$$H_{eff} = -\frac{\theta}{2}(\omega_I I_y + \omega_S S_y) + 2\pi J I_z S_z \quad (11)$$

We have produced an effective rf-field that is perpendicular to the coupling interactions. This will decouple the spins. When we go in the interaction frame of $(\omega_I I_y + \omega_S S_y)$, all coupling is eliminated.

The pulse sequence for producing the desired effective Hamiltonian is shown in figure. 1

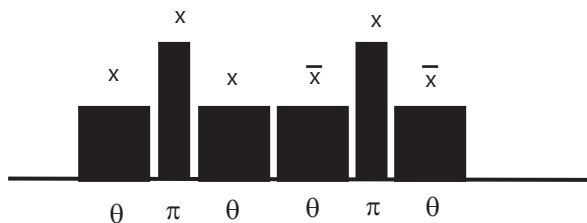
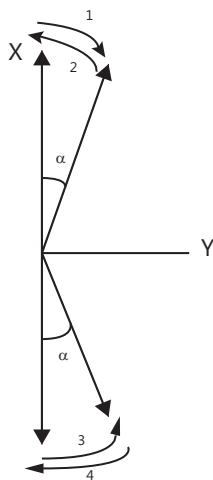


Figure 1: The figure shows the pulse sequence for synthesizing an effective y field used for spin decoupling.

How does the rf Hamiltonian evolve in the toggling frame of the chemical shift is depicted in figure 2.



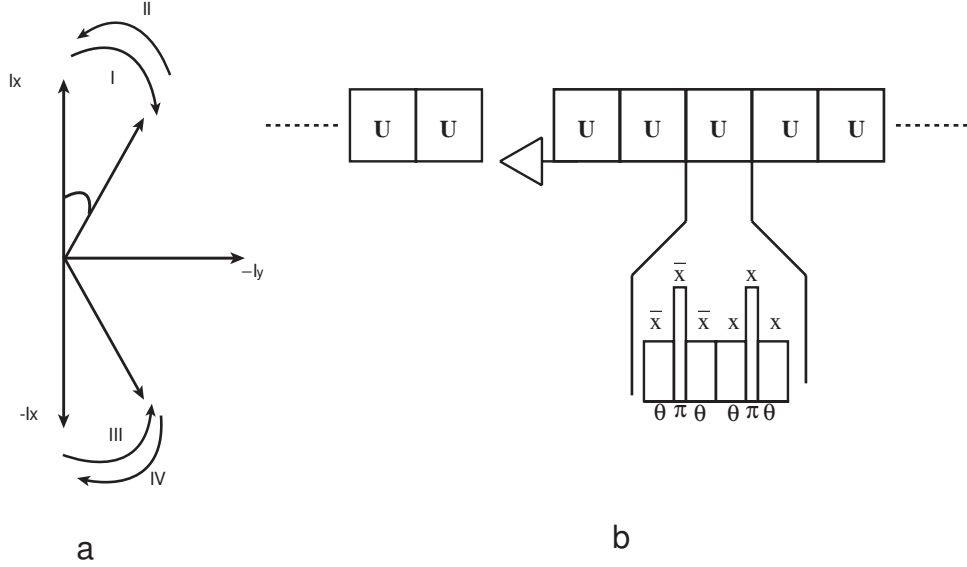
We apply this building block depicted in figure 1 and sample a point from FID (free induction decay) and repeat. The prototype of the basic experiment is shown in

We have calculated the effective Hamiltonian to first order in θ . We we calculate it to second order in the theta we find the effective Hamiltonian

$$\exp(-iH_{eff}4\Delta) = \exp(-iH_4\Delta) \exp(-iH_3\Delta) \exp(-iH_2\Delta) \exp(-iH_1\Delta) \quad (12)$$

can be calculated using $\exp(A) \exp(B) = \exp(A + B + \frac{[A,B]}{2} + \frac{[A[A,B]] + [A,B]B}{12} + \dots)$.

This gives



$$H_{eff}4\Delta = -2\theta(\omega_I I_y + \omega_S S_y)\Delta + 2\theta^2(\omega_I I_z + \omega_S S_z)\Delta + 2\pi J\Delta(4I_z S_z + 4\theta(I_y S_z + I_z S_y)) + \frac{16}{3}\theta^2 I_y S_y \quad (13)$$

The effective field instead of being along y is along direction $I_{y'} = -I_y + \theta I_z$ and $S_{y'} = -S_y + \theta S_z$ respectively. We resolve the coupling along this direction keeping only the parallel part of the coupling with the effective field. This parallel coupling is

$$4J_{\parallel} = 2\pi J\Delta(4\theta^2 - 8\theta^2 + \frac{16}{3}\theta^2)I_{y'}S_{y'} \quad (14)$$

Therefore the effective Hamiltonian is

$$H_{eff} = \frac{\theta}{2}(\omega_I I_{y'} + \omega_S S_{y'}) + 2\pi J\frac{\theta^2}{3}I_{y'}S_{y'} \quad (15)$$

Therefore a part of the coupling stays and reflects itself as an envelop in Fig. 2, where we show how the magnetization on spin I evolves when we donot decouple (blue curve) vs when we apply our decoupling sequence (red curve). When no decoupling is performed, magnetization evolves to spin S and we see a coupling evolution. When we apply decoupling sequence, the magnetization on spin I stays

The pulse sequence in Fig. 1 applies rf-field at the same time as coupling and

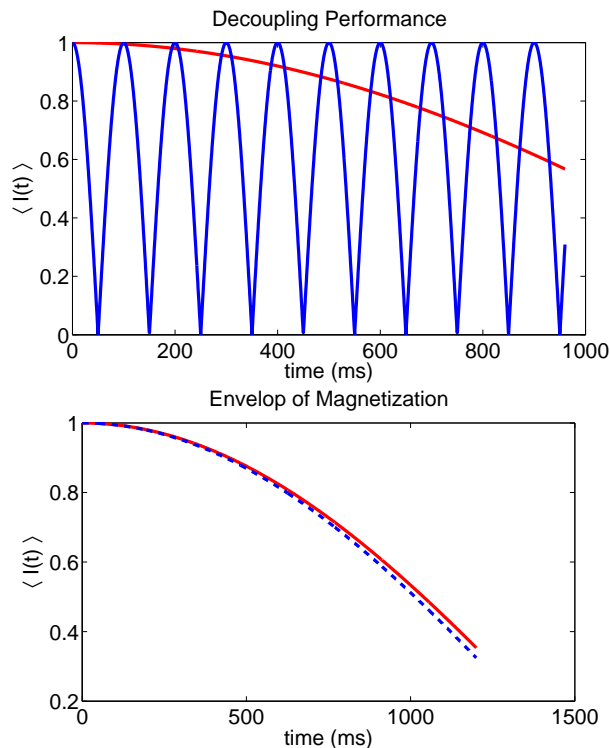


Figure 2: The top figure shows how magnetization $\langle I(t) \rangle = \sqrt{\langle I_x(t) \rangle^2 + \langle I_y(t) \rangle^2 + \langle I_z(t) \rangle^2}$ on spin I evolves when we donot decouple (blue curve) vs when we apply the decoupling sequence in Fig. 1 (red curve). The decoupling of spins results in magnetization of spin I staying on spin I . Here, $\frac{\omega_I}{2\pi} = 2400$ Hz, $\frac{\omega_S}{2\pi} = 800$ Hz, $J = 10$ Hz, $\frac{A}{2\pi} = 5000$ Hz and $\theta = \frac{\pi}{10}$. Bottom figure compares the envelop of magnetization of spin I (red curve) with the calculated value as in Eq. 15 (blue curve).

chemical shift evolution resulting. It is possible to engineer the same effective Hamiltonian if we apply a hard rf-pulse of flip angle θ followed by a delay in which coupling and chemical shift evolve. In nutshell the evolution

$$\exp(-i(\omega_I I_z + \omega_S S_z + 2\pi J I_z S_z + A F_x) \Delta) \sim \exp(-i(\omega_I I_z + \omega_S S_z + 2\pi J I_z S_z) \Delta) \exp(-i F_x \theta) \quad (16)$$

is approximated by pulse and evolution as above. We can now write the pulse sequence as

$$U = U_4 U_3 U_2 U_1 \quad (17)$$

$$U_1 = \exp(-i(\omega_I I_z + \omega_S S_z + 2\pi J I_z S_z)\Delta) \exp(-iF_x \theta) \quad (18)$$

$$U_2 = \exp(-i(-\omega_I I_z - \omega_S S_z + 2\pi J I_z S_z)\Delta) \exp(-iF_x \theta) \quad (19)$$

$$U_3 = \exp(-i(-\omega_I I_z - \omega_S S_z + 2\pi J I_z S_z)\Delta) \exp(iF_x \theta) \quad (20)$$

$$U_4 = \exp(-i(\omega_I I_z + \omega_S S_z + 2\pi J I_z S_z)\Delta) \exp(iF_x \theta) \quad (21)$$

The pulse sequence for producing the desired effective evolution is given in Fig. 3

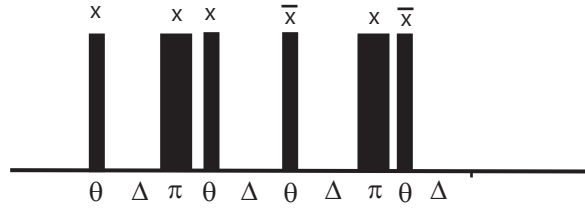


Figure 3: The figure shows the pulse sequence for synthesizing an effective y field constructed from pulses and delays.

We can now calculate the effective Hamiltonian for this pulse sequence.

$$\exp(-iH_{eff}4\Delta) = U_4 U_3 U_2 U_1 \quad (22)$$

can be calculated using $\exp(A) \exp(B) = \exp(A + B + \frac{[A,B]}{2} + \frac{[A[A,B]] + [[A,B]B]}{12} + \dots)$.

This gives

$$H_{eff}4\Delta = -2\theta(\omega_I I_y + \omega_S S_y)\Delta + 2\theta^2(\omega_I I_z + \omega_S S_z)\Delta + 2\pi J\Delta(4I_z S_z + 4\theta(I_y S_z + I_z S_y)) + \frac{18}{3}\theta^2 I_y S_y \quad (23)$$

The effective field instead of being along y is along direction $I_{y'} = -I_y + \theta I_z$ and $S_{y'} = -S_y + \theta S_z$ respectively. We resolve the coupling along this direction keeping only the parallel part of the coupling with the effective field. This parallel coupling is

$$4J_{\parallel} = 2\pi J\Delta(4\theta^2 - 8\theta^2 + \frac{18}{3}\theta^2)I_{y'}S_{y'} \quad (24)$$

Therefore the effective Hamiltonian is

$$H_{eff} = \frac{\theta}{2}(\omega_I I_{y'} + \omega_S S_{y'}) + 2\pi J \frac{\theta^2}{2} I_{y'} S_{y'} \quad (25)$$

Therefore a part of the coupling stays and reflects itself as an envelop in Fig. 4, where we show how the magnetization on spin I evolves when we donot decouple (blue curve) vs when we apply our decoupling sequence (red curve). When no decoupling is performed, magnetization evolves to spin S and we see a coupling evolution. When we apply decoupling sequence, the magnetization on spin I stays

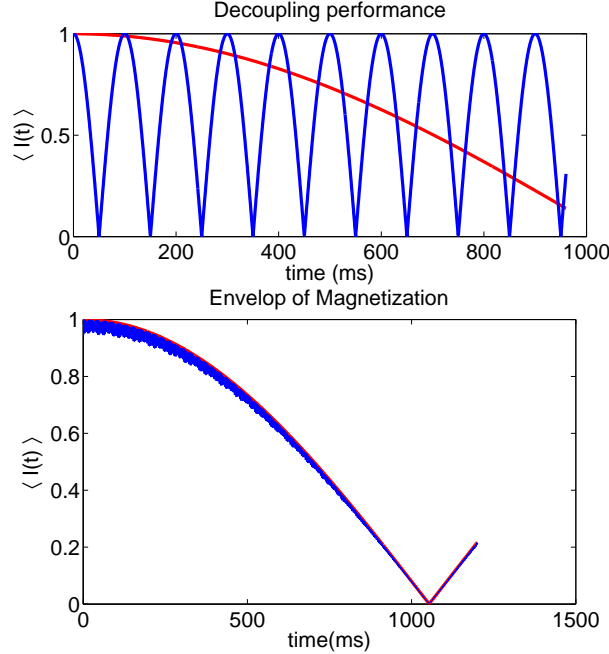


Figure 4: The top figure shows how magnetization on spin I evolves when we donot decouple (blue curve) vs when we apply the decoupling sequence in Fig. 1 (red curve). The decoupling of spins results in magnetization of spin I staying on spin I . Here, $\frac{\omega_I}{2\pi} = 2400$ Hz, $\frac{\omega_S}{2\pi} = 800$ Hz, $J = 10$ Hz, $\frac{A}{2\pi} = 5000$ Hz and $\theta = \frac{\pi}{10}$. Bottom figure compares the envelop of magnetization of spin I (red curve) with the calculated value as in Eq. 25 (blue curve).

In the pulse sequences presented in Fig. 1 and Fig. 3, we produce an effective y field with scaling of chemical shift by a factor $\frac{\theta}{2}$. We now show how by using pulses and delays in our pulses sequence, we can improve this scaling factor to θ . Let

$$U = U_4 U_3 U_2 U_1 \quad (26)$$

$$U_1 = \exp(-iF_x\theta) \exp(-i(\omega_I I_z + \omega_S S_z + 2\pi J I_z S_z)\Delta) \quad (27)$$

$$U_2 = \exp(-i(-\omega_I I_z - \omega_S S_z + 2\pi J I_z S_z)\Delta) \exp(-iF_x\theta) \quad (28)$$

$$U_3 = \exp(-iF_x\theta) \exp(-i(-\omega_I I_z - \omega_S S_z + 2\pi J I_z S_z)\Delta) \quad (29)$$

$$U_4 = \exp(-i(\omega_I I_z + \omega_S S_z + 2\pi J I_z S_z)\Delta) \exp(iF_x\theta) \quad (30)$$

The pulse sequence for producing the desired effective evolution is given in Fig. 5

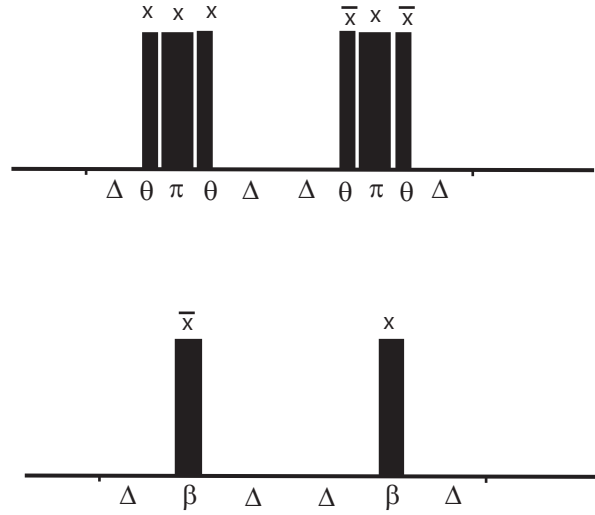


Figure 5: The figure shows the pulse sequence for synthesizing an effective y field used for spin decoupling. The pulse sequence enhances the resolution of chemical shifts by a factor of 2 over the sequence in 1.

We can now calculate the effective Hamiltonian for this pulse sequence.

$$\exp(-iH_{eff}4\Delta) = U_4 U_3 U_2 U_1 \quad (31)$$

$$H_{eff}4\Delta = -4\theta(\omega_I I_y + \omega_S S_y)\Delta + 4\theta^2(\omega_I I_z + \omega_S S_z)\Delta + 2\pi J\Delta(4I_z S_z + 4\theta(I_y S_z + I_z S_y)) + \frac{24}{3}\theta^2 I_y S_y \quad (32)$$

This parallel coupling is

$$4J_{\parallel} = 2\pi J\Delta(4\theta^2 - 8\theta^2 + \frac{24}{3}\theta^2)I_{y'}S_{y'} \quad (33)$$

Therefore the effective Hamiltonian is

$$H_{eff} = \theta(\omega_I I_{y'} + \omega_S S_{y'}) + 2\pi J\theta^2 I_{y'} S_{y'} \quad (34)$$

Therefore a part of the coupling stays and reflects itself as an envelop in Fig. 6, where we show how the magnetization on spin I evolves when we donot decouple (blue curve) vs when we apply our decoupling sequence (red curve). When no decoupling is performed, magnetization evolves to spin S and we see a coupling evolution. When we apply decoupling sequence, the magnetization on spin I stays

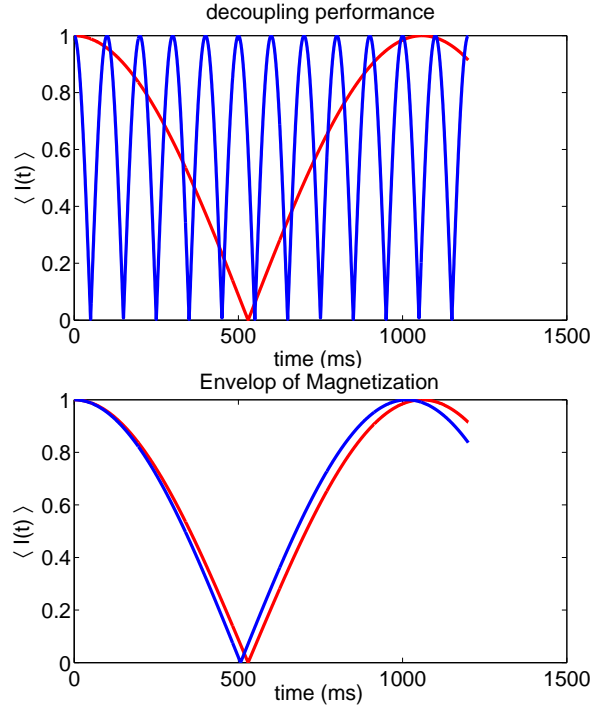


Figure 6: The top figure shows how magnetization on spin I evolves when we donot decouple (blue curve) vs when we apply the decoupling sequence in Fig. 5(red curve). The decoupling of spins results in magnetization of spin I staying on spin I . Here, $\frac{\omega_I}{2\pi} = 2400$ Hz, $\frac{\omega_S}{2\pi} = 800$ Hz, $J = 10$ Hz, $\frac{A}{2\pi} = 5000$ Hz and $\theta = \frac{\pi}{10}$. Bottom figure compares the envelop of magnetization of spin I (red curve) with the calculated value as in Eq. 34 (blue curve).

The pulse sequences we have presented use four decoupling stages for decoupling the Ising coupling. Here we show how we can do this just using two decoupling stages.

Let

$$U = U_2 U_1 \quad (35)$$

$$U_1 = \exp(-i(\omega_I I_z + \omega_S S_z + 2\pi J I_z S_z)\Delta) \exp(-iF_x \theta) \quad (36)$$

$$U_2 = \exp(-i(-\omega_I I_z - \omega_S S_z + 2\pi J I_z S_z)\Delta) \exp(iF_x \theta) \quad (37)$$

The pulse sequence for producing the desired effective evolution is given in Fig. 7

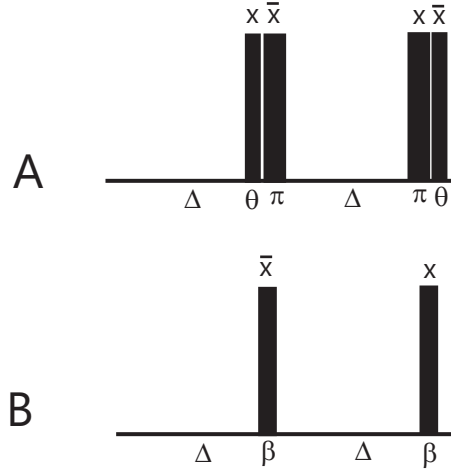


Figure 7: The figure shows the pulse sequence for synthesizing an effective y field used for spin decoupling. The pulse sequence uses only two evolution stages. Pulse B above simplifies Pulse A.

We can now calculate the effective Hamiltonian for this pulse sequence.

$$\exp(-iH_{eff}4\Delta) = U_2 U_1 \quad (38)$$

$$\begin{aligned}
H_{eff}2\Delta &= -\theta(\omega_I I_y + \omega_S S_y)\Delta + \frac{\theta}{2}(\omega_I \theta I_z - \Delta \omega_I^2 I_x)\Delta + \frac{\theta}{2}(\omega_S \theta S_z - \Delta \omega_S^2 S_x)\Delta \\
&\quad 2\pi J\Delta(2I_z S_z + 2\theta(I_y S_z + I_z S_y) + \theta^2 I_y S_y)
\end{aligned} \tag{40}$$

The effective field is along direction

$$I_\alpha = -I_y + \frac{1}{2}(\theta I_z - \omega_I \Delta I_x) \tag{41}$$

$$S_\beta = -S_y + \frac{1}{2}(\theta S_z - \omega_S \Delta S_x) \tag{42}$$

This parallel coupling is

$$2J_{\parallel} = 2\pi J\Delta\left(\frac{\theta^2}{2} - \theta^2 + \theta^2\right)I_\alpha S_\beta \tag{43}$$

Therefore the effective Hamiltonian is

$$H_{eff} = \theta(\omega_I I_\alpha + \omega_S S_\beta) + 2\pi J\frac{\theta^2}{4}I_\alpha S_\beta \tag{44}$$

Therefore a part of the coupling stays and reflects itself as an envelop in Fig. 8, where we show how the magnetization on spin I evolves when we donot decouple (blue curve) vs when we apply our decoupling sequence (red curve). When no decoupling is performed, magnetization evolves to spin S and we see a coupling evolution. When we apply decoupling sequence, the magnetization on spin I stays

3 Isotropic Couplings

Until now we considered coupling between the spins as Ising coupling. Now we consider the case of Isotropic coupling, when the coupling Hamiltonian has the form

$$I \cdot S = I_x S_x + I_y S_y + I_z S_z \tag{45}$$

Under the pulse sequence in in Fig. 1, we see how this coupling Hamiltonian evolve in the toggling frame of the chemical shifts. When chemical shifts goes through a

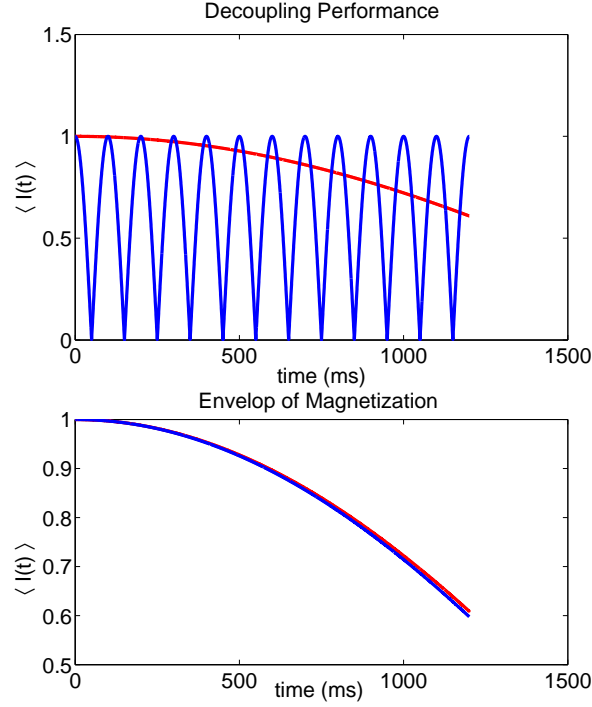


Figure 8: The top figure shows how magnetization on spin I evolves when we donot decouple (blue curve) vs when we apply the decoupling sequence in Fig. 7(red curve). The decoupling of spins results in magnetization of spin I staying on spin I . Here, $\frac{\omega_I}{2\pi} = 2400$ Hz, $\frac{\omega_S}{2\pi} = 800$ Hz, $J = 10$ Hz, $\frac{A}{2\pi} = 5000$ Hz and $\theta = \frac{\pi}{10}$. Bottom figure compares the envelop of magnetization of spin I (red curve) with the calculated value as in Eq. 44 (blue curve)

evolution $(\omega_I I_z + \omega_S S_z)\Delta$, $-(\omega_I I_z + \omega_S S_z)\Delta$, $-(\omega_I I_z + \omega_S S_z)\Delta$, $(\omega_I I_z + \omega_S S_z)\Delta$, the planar part of the coupling $I_x S_x + I_y S_y$ evolves as

$$I_x S_x + I_y S_y \rightarrow (I_x S_x + I_y S_y) \cos(\omega_I - \omega_S)t + (I_x S_y - I_y S_x) \sin(\omega_I - \omega_S)t = J_1(t)$$

$$I_x S_x + I_y S_y \rightarrow (I_x S_x + I_y S_y) \cos(\omega_I - \omega_S)\Delta - t + (I_x S_y - I_y S_x) \sin(\omega_I - \omega_S)\Delta - t = J_2(t)$$

$$I_x S_x + I_y S_y \rightarrow (I_x S_x + I_y S_y) \cos(\omega_I - \omega_S)t - (I_x S_y - I_y S_x) \sin(\omega_I - \omega_S)t = J_3(t)$$

$$I_x S_x + I_y S_y \rightarrow (I_x S_x + I_y S_y) \cos(\omega_I - \omega_S)\Delta - t - (I_x S_y - I_y S_x) \sin(\omega_I - \omega_S)\Delta - t = J_4(t)$$

All of this then sums to an effective evolution $\int_0^\Delta J_1(t) + J_2(t) + J_3(t) + J_4(t)dt$,

$$\frac{4(I_x S_x + I_y S_y) \sin(\omega_I - \omega_S)\Delta}{\omega_I - \omega_S} \quad (46)$$

The effective rf-field produced by the pulse sequence in Fig. 1, is along y direction. This effective field will not decouple the yy part of the Hamiltonian in 46. Therefore we donot get complete decoupling. This is shown in top figure 9.

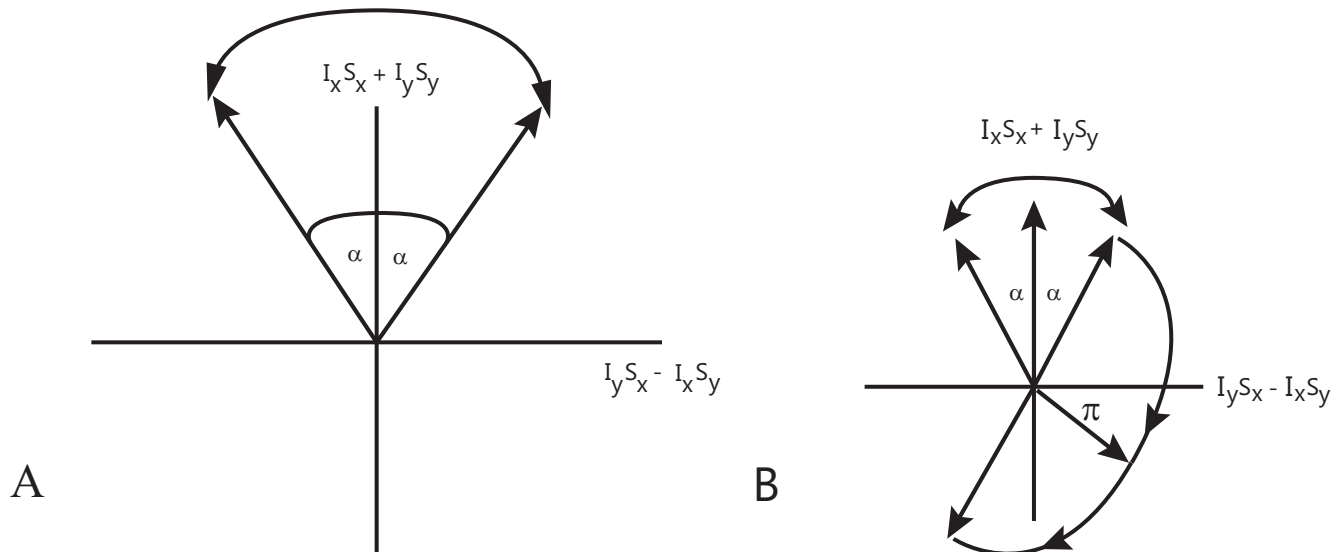


Figure 9: The top figure shows how the planar part of the Isotropic coupling Hamiltonian evolves under the four cycle of Fig. 1. Bottom figure shows how planar part is averaged by introducing more stages in the pulse sequence shown in figure 10.

To eliminate the yy part of the Hamiltonian we propose the following pulse sequence in Fig. 10, where $\tau = \frac{\pi}{\omega_I - \omega_S}$ and $\alpha = (\omega_I - \omega_S)\Delta$.

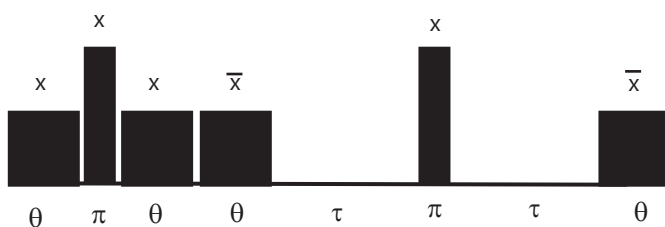


Figure 10: The top figure is a six stage pulse sequence to decouple Isotropic coupling Hamiltonian.

We analyze the six stage pulse sequence formed out of Hamiltonians. The evolution of the planar Hamiltonian under these set of Hamiltonians is shown in bottom figure 9.

$$H_1 = \omega_I I_z + \omega_S S_z + 2\pi J I \cdot S + AF_x \quad (47)$$

$$H_2 = -\omega_I I_z - \omega_S S_z + 2\pi J I \cdot S + AF_x \quad (48)$$

$$H_3 = -\omega_I I_z - \omega_S S_z + 2\pi J I \cdot S - AF_x \quad (49)$$

$$H_4 = -\omega_I I_z - \omega_S S_z + 2\pi J I \cdot S \quad (50)$$

$$H_5 = \omega_I I_z + \omega_S S_z + 2\pi J I \cdot S \quad (51)$$

$$H_6 = \omega_I I_z + \omega_S S_z + 2\pi J I \cdot S - AF_x \quad (52)$$

Under this pulse sequence , to first order the planar Hamiltonian averages to

$$\frac{4(I_y S_x - I_x S_y) \cos(\omega_I - \omega_S) \Delta}{\omega_I - \omega_S} \quad (53)$$

and the effective rf field Hamiltonian to first order in θ is as in $1 \frac{\theta}{2}(\omega_I I_y + \omega_S S_y)$. This effective rf-Hamiltonian will remove the averaged Isotropic coupling and we get decoupling. We can evaluate the effect of the pulse sequence in 10 to higher order in θ

$$U = \exp(-iH_6\Delta) \exp(-iH_5\tau) \exp(-iH_4\tau) \exp(-iH_3\Delta) \exp(-iH_2\Delta) \exp(-iH_1\Delta). \quad (54)$$

The effective Hamiltonian can now be evaluated. First observe , by evaluating in the toggling frame of the chemical shift we find

$$\exp(-iH_5\tau) \exp(-iH_4\tau) = \exp(-i\frac{4\pi J \Delta}{\alpha}(2I_y S_x - 2I_x S_y + \pi I_z S_z)) = \exp(-iJ_I \Delta)$$

Then the evolution

$$U = \exp(-iH_6\Delta) \exp(-iJ_I \Delta) \exp(-iH_3\Delta) \exp(-iH_2\Delta) \exp(-iH_1\Delta) \quad (55)$$

$$= \exp(-i\tilde{J}_I \Delta) \exp(-iH_6\Delta) \exp(-iH_3\Delta) \exp(-iH_2\Delta) \exp(-iH_1\Delta) \quad (56)$$

where

$$\tilde{J}_I = \exp(-iH_6\Delta)J_I \exp(iH_6\Delta) \quad (57)$$

Under this transformation

$$I_y S_x - I_x S_y \rightarrow I_y S_x - I_x S_y - \alpha(I_x S_x + I_y S_y) \quad (58)$$

$$I_z S_z \rightarrow I_z S_z + (I_z S_y + I_y S_z)\theta \quad (59)$$

In Eq. 55, we have already solved for the evolution

$$\exp(-iH_{eff}4\Delta) = \exp(-iH_6\Delta) \exp(-iH_3\Delta) \exp(-iH_2\Delta) \exp(-iH_1\Delta) \quad (60)$$

in Eq. 15. The result can be modified for isotropic coupling to

$$H_{eff} = \frac{\theta}{2}(\omega_I I_{y'} + \omega_S S_{y'}) + 2\pi J(I \cdot S - \frac{\alpha^2}{6}(I_x S_x + I_y S_y)) \quad (61)$$

Combining eq. 55 with 58 and 61, we are left with an effective coupling which is

$$H_{eff} = \frac{\theta}{2}(\omega_I I_{y'} + \omega_S S_{y'}) - 2\pi J(\frac{\theta^2}{2} + \frac{\alpha^2}{6})I_{y'} S_{y'} \quad (62)$$

Therefore a part of the coupling stays and reflects itself as an envelop in Fig. 11, where we show how the magnetization on spin I evolves when we donot decouple (blue curve) vs when we apply our decoupling sequence (red curve). When no decoupling is performed, magnetization evolves to spin S and we see a coupling evolution. When we apply decoupling sequence, the magnetization on spin I stays

When we studied the four stage pulse sequence in Fig. 1, we showed it can be implemented in two other ways presented in Fig. 3 and 5, where we use pulses and

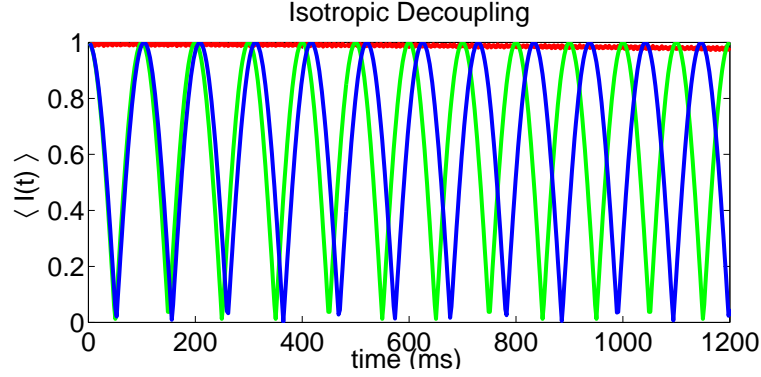


Figure 11: The top figure shows how magnetization on spin I evolves when we don't decouple (green curve) vs when we apply the four stage decoupling sequence in Fig. 1 (blue curve) and finally the six stage pulse sequence (red curve) of Fig. 10. The decoupling of spins results in magnetization of spin I staying on spin I . Here, $\frac{\omega_I}{2\pi} = 2400$ Hz, $\frac{\omega_S}{2\pi} = 800$ Hz, $J = 10$ Hz, $\frac{A}{2\pi} = 1000$ Hz and $\theta = \frac{\pi}{10}$

delays. For decoupling isotropic interactions, the six stage pulse sequence of Fig. 10 can also be implemented in two other ways. We present there other methods now.

Consider the pulse sequence in the following Fig. 12, where we have six stages in the evolution.

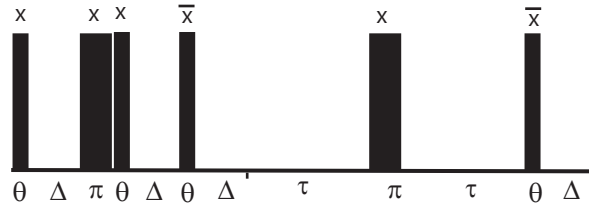


Figure 12: The top figure is a six stage pulse sequence to decouple Isotropic coupling Hamiltonian.

We analyze the six stage pulse sequence formed out of Hamiltonians. Here $\tau = \frac{1}{2(\omega_I - \omega_S)}$.

$$U_1 = \exp(-i\Delta(\omega_I I_z + \omega_S S_z + 2\pi JI \cdot S)) \exp(-i\Delta A F_x) \quad (63)$$

$$U_2 = \exp(-i\Delta(-\omega_I I_z - \omega_S S_z + 2\pi JI \cdot S)) \exp(-i\Delta A F_x) \quad (64)$$

$$U_1 = \exp(-i\Delta(-\omega_I I_z - \omega_S S_z + 2\pi JI \cdot S)) \exp(i\Delta A F_x) \quad (65)$$

$$U_1 = \exp(-i\tau(-\omega_I I_z - \omega_S S_z + 2\pi JI \cdot S)) \quad (66)$$

$$U_1 = \exp(-i\tau(\omega_I I_z + \omega_S S_z + 2\pi JI \cdot S)) \quad (67)$$

$$U_1 = \exp(-i\Delta(\omega_I I_z + \omega_S S_z + 2\pi JI \cdot S)) \exp(i\Delta A F_x) \quad (68)$$

The total evolution is

$$U = U_6 U_5 U_4 U_3 U_2 U_1 \quad (69)$$

The effective Hamiltonian of this pulse sequence is

$$H_{eff} = \frac{\theta}{2}(\omega_I I_{y'} + \omega_S S_{y'}) - 2\pi J \left(\frac{\alpha^2}{6}\right) I_{y'} S_{y'} \quad (70)$$

Therefore a part of the coupling stays and reflects itself as an envelop in Fig. 13, where we show how the magnetization on spin I evolves when we donot decouple (blue curve) vs when we apply our decoupling sequence (red curve). When no decoupling is performed, magnetization evolves to spin S and we see a coupling evolution. When we apply decoupling sequence, the magnetization on spin I stays

Now we can again improve the scaling factor of the chemical shifts by changing the order of pulses and delays. Consider the pulse sequence in the following Fig. 14, where we have six stages in the evolution.

We analyze the six stage pulse sequence formed out of Hamiltonians. Here $\tau = \frac{1}{2(\omega_I - \omega_S)}$.

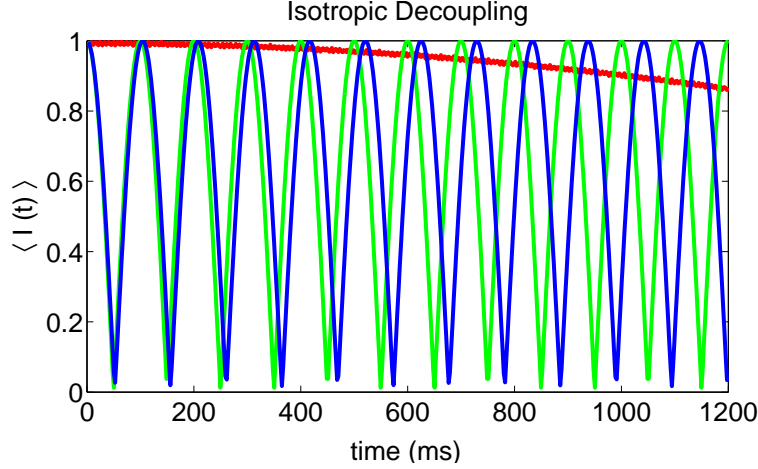


Figure 13: The top figure shows how magnetization on spin I evolves when we don't decouple (green curve) vs when we apply the four stage decoupling sequence in Fig. 1(blue curve) and finally the six stage pulse sequence (red curve) of Fig. 12. The decoupling of spins results in magnetization of spin I staying on spin I . Here, $\frac{\omega_I}{2\pi} = 2400$ Hz, $\frac{\omega_S}{2\pi} = 800$ Hz, $J = 10$ Hz, $\frac{A}{2\pi} = 1000$ Hz and $\theta = \frac{\pi}{10}$

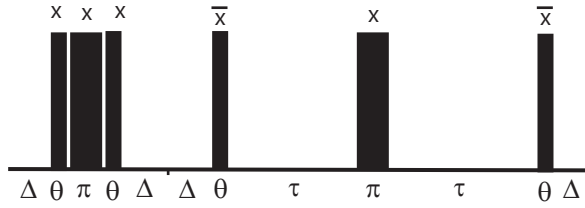


Figure 14: The top figure is a six stage pulse sequence to decouple Isotropic coupling Hamiltonian.

$$U_1 = \exp(-i\Delta AF_x) \exp(-i\Delta(\omega_I I_z + \omega_S S_z + 2\pi J I \cdot S)) \quad (71)$$

$$U_2 = \exp(-i\Delta(-\omega_I I_z - \omega_S S_z + 2\pi J I \cdot S)) \exp(-i\Delta AF_x) \quad (72)$$

$$U_1 = \exp(i\Delta AF_x) \exp(-i\Delta(-\omega_I I_z - \omega_S S_z + 2\pi J I \cdot S)) \quad (73)$$

$$U_1 = \exp(-i\tau(-\omega_I I_z - \omega_S S_z + 2\pi J I \cdot S)) \quad (74)$$

$$U_1 = \exp(-i\tau(\omega_I I_z + \omega_S S_z + 2\pi J I \cdot S)) \quad (75)$$

$$U_1 = \exp(-i\Delta(\omega_I I_z + \omega_S S_z + 2\pi J I \cdot S)) \exp(i\Delta AF_x) \quad (76)$$

The total evolution is

$$U = U_6 U_5 U_4 U_3 U_2 U_1 \quad (77)$$

The effective Hamiltonian of this pulse sequence is

$$H_{eff} = \theta(\omega_I I_{y'} + \omega_S S_{y'}) - 2\pi J \left(\frac{\alpha^2}{6}\right) I_{y'} S_{y'} \quad (78)$$

Therefore a part of the coupling stays and reflects itself as an envelop in Fig. 13, where we show how the magnetization on spin I evolves when we donot decouple (blue curve) vs when we apply our decoupling sequence (red curve). When no decoupling is performed, magnetization evolves to spin S and we see a coupling evolution. When we apply decoupling sequence, the magnetization on spin I stays

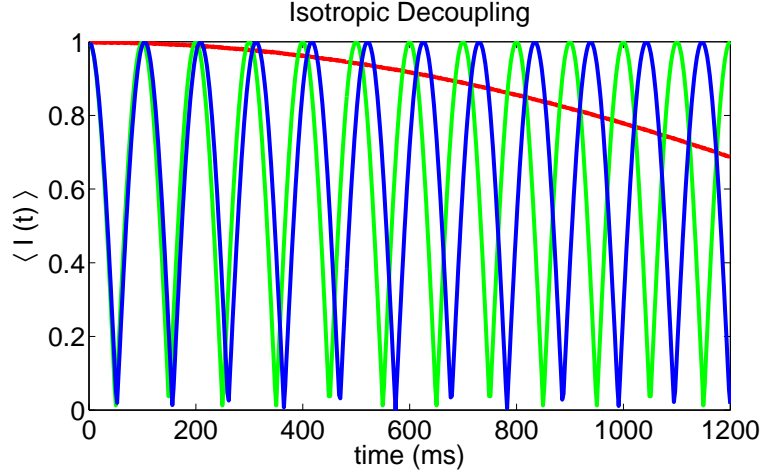


Figure 15: The top figure shows how magnetization on spin I evolves when we donot decouple (green curve) vs when we apply the four stage decoupling sequence in Fig. 1(blue curve) and finally the six stage pulse sequence (red curve) of Fig. 14. The decoupling of spins results in magnetization of spin I staying on spin I . Here, $\frac{\omega_I}{2\pi} = 2400$ Hz, $\frac{\omega_S}{2\pi} = 800$ Hz, $J = 10$ Hz, $\frac{A}{2\pi} = 1000$ Hz and $\theta = \frac{\pi}{10}$

Until now we have used a six stage pulse sequence to decouple Isotropic coupling. We now show how the four stage pulse sequence in Fig. 1 can be used to decouple isotropic coupling. In the four stage pulse sequence in Fig. 1, we choose the time $\Delta = \frac{\pi}{\omega_I - \omega_S}$. Since the evolution time Δ is made large, in the toggling frame of the chemical shifts we make large excursion/dip. We consider the evolution of the Hamiltonians in Eq. 2-5, in the toggling frame of the chemical shifts. Let $\tau = \Delta - t$

$$\tilde{H}_1(t) = \exp(i(\omega_I I_z + \omega_S S_z)t)(2\pi JI \cdot S + AF_x) \exp(-i(\omega_I I_z + \omega_S S_z)t) \quad (79)$$

$$\tilde{H}_2(t) = \exp(-i(\omega_I I_z + \omega_S S_z)\tau)(2\pi JI \cdot S + AF_x) \exp(i(\omega_I I_z + \omega_S S_z)\tau) \quad (80)$$

$$\tilde{H}_3(t) = \exp(-i(\omega_I I_z + \omega_S S_z)t)(2\pi JI \cdot S - AF_x) \exp(i(\omega_I I_z + \omega_S S_z)t) \quad (81)$$

$$\tilde{H}_4(t) = \exp(i(\omega_I I_z + \omega_S S_z)\tau)(2\pi JI \cdot S - AF_x) \exp(-i(\omega_I I_z + \omega_S S_z)\tau) \quad (82)$$

We produce the evolution

$$\exp(-iH_{eff}4\Delta) = U = \tilde{U}_4\tilde{U}_3\tilde{U}_2\tilde{U}_1 \quad (83)$$

where, $\tilde{U}_i = \exp(A_i + B_i + C_i)$

$$A_i = -i \int_0^\Delta \tilde{H}_i(\sigma_1) d\sigma_1 \quad (84)$$

$$B_i = - \int_0^\Delta \int_0^{\sigma_1} [\tilde{H}_i(\sigma_1), \tilde{H}_i(\sigma_2)] d\sigma_2 d\sigma_1 \quad (85)$$

$$C_i = i \int_0^\Delta \int_0^{\sigma_1} \int_0^{\sigma_2} [\tilde{H}_i(\sigma_1)[\tilde{H}_i(\sigma_2), \tilde{H}_i(\sigma_3)]] + [[\tilde{H}_i(\sigma_1), \tilde{H}_i(\sigma_2)]\tilde{H}_i(\sigma_3)] d\sigma_3 d\sigma_2 d\sigma_1$$

Under large dip, the planar part of the coupling evolves in the toggling frame of the chemical shifts as shown in figure 16 and averages out.

The effective Hamiltonian in Eq. 83, takes the following form, where $\theta = A\Delta$,

$$\begin{aligned} H_{eff} = & -\frac{\theta}{2} \left(\left(\frac{\sin \frac{\omega_I \Delta}{2}}{\frac{\omega_I \Delta}{2}} \right)^2 \omega_I I_y + \left(\frac{\sin \frac{\omega_S \Delta}{2}}{\frac{\omega_S \Delta}{2}} \right)^2 \omega_S S_y \right) + \frac{\theta^2}{2} \left(\left(\frac{\sin \frac{\omega_I \Delta}{2}}{\frac{\omega_I \Delta}{2}} \right)^2 \left(\frac{\sin \omega_I \Delta}{\omega_I \Delta} \right) \omega_I I_z \right. \\ & \left. + \left(\frac{\sin \frac{\omega_S \Delta}{2}}{\frac{\omega_S \Delta}{2}} \right)^2 \left(\frac{\sin \omega_S \Delta}{\omega_S \Delta} \right) \omega_S S_z \right) + 2\pi J \theta^2 \left(\frac{1}{3} \frac{\sin \omega_I \Delta}{\omega_I \Delta} \frac{\sin \omega_S \Delta}{\omega_S \Delta} + f(\omega_I, \omega_S) \right) I_y S_y. \end{aligned}$$

where,

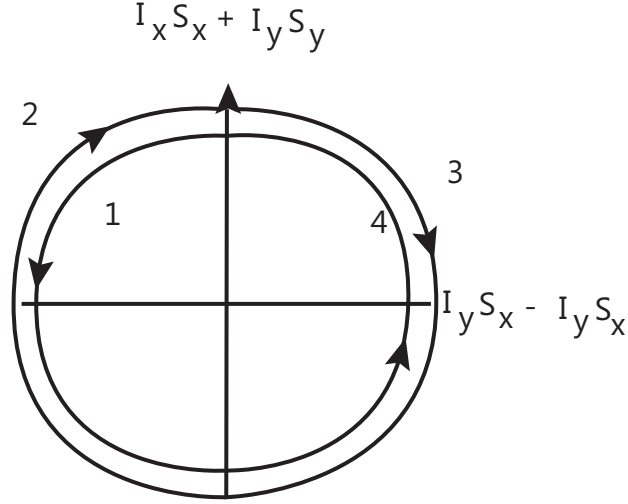


Figure 16: The top figure shows how planar part of the coupling evolves under four stage pulse sequence in Eq. 79.

$$\begin{aligned}
 f(\omega_I, \omega_S) &= \frac{1}{4(\omega_S \Delta)^2} \left(\frac{\sin(\omega_I + \omega_S) \Delta}{(\omega_I + \omega_S) \Delta} + \frac{\sin(\omega_I - \omega_S) \Delta}{(\omega_I - \omega_S) \Delta} \right) + \frac{1}{4(\omega_I \Delta)^2} \left(\frac{\sin(\omega_I + \omega_S) \Delta}{(\omega_I + \omega_S) \Delta} \right. \\
 &+ \left. \frac{\sin(\omega_S - \omega_I) \Delta}{(\omega_S - \omega_I) \Delta} \right) - \frac{1}{2(\omega_S \Delta)^2} \frac{\sin \omega_I \Delta}{\omega_I \Delta} - \frac{1}{2(\omega_I \Delta)^2} \frac{\sin \omega_S \Delta}{\omega_S \Delta} + \frac{1}{6} \frac{\sin \omega_I \Delta}{\omega_I \Delta} \frac{\sin \omega_S \Delta}{\omega_S \Delta}
 \end{aligned}$$

Therefore a part of the coupling stays and reflects itself as an envelop in Fig. 17, where we show how the magnetization on spin I evolves when we donot decouple (blue curve) vs when we apply our decoupling sequence (red curve). When no decoupling is performed, magnetization evolves to spin S and we see a coupling evolution. When we apply decoupling sequence, the magnetization on spin I stays

In this paper we studied the problem of homonuclear decoupling. We first analyzed the case of Ising coupling and developed a four stage pulse sequence to decouple this interaction and measure chemical shifts. We then looked at Isotropic Hamiltonian and showed how the four stage sequence had to be modified to a six stage pulse sequence to decouple isotropic coupling. We presented calculations and simulations to show the effectiveness of decoupling sequences.

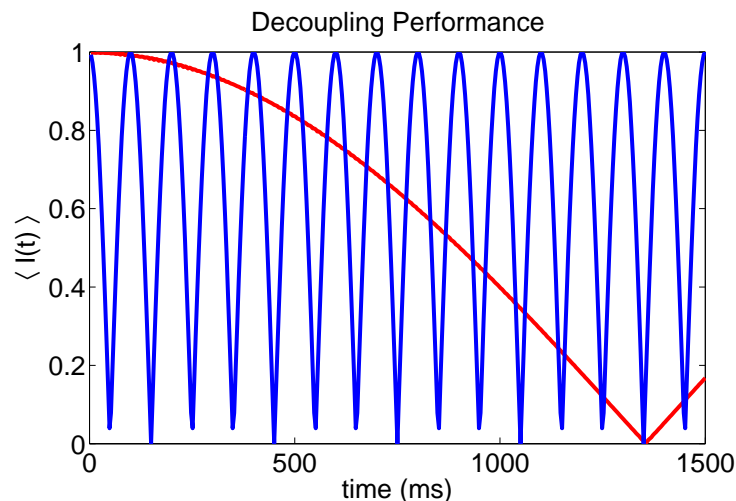


Figure 17: The top figure shows how magnetization on spin I evolves when we don't decouple (green curve) vs when we apply the four stage decoupling sequence in Fig. 1 with large dip angle (red curve). The decoupling of spins results in magnetization of spin I staying on spin I . Here, $\frac{\omega_I}{2\pi} = 2400$ Hz, $\frac{\omega_S}{2\pi} = 800$ Hz, $J = 10$ Hz, $\frac{A}{2\pi} = 200$ Hz and $\theta = \frac{\pi}{8}$

References

- [1] R. Ernst, G. Bodenhausen, and A. Wokaun, Principles of Nuclear Magnetic Resonance in One and Two Dimensions (Clarendon, 1987).
- [2] Freeman, Spin Choreography: Basic Steps in High Resolution NMR (Oxford University Press, 1998).
- [3] A. J. Shaka, J. Keeler, and R. Freeman, "Evaluation of a new broadband decoupling sequence: WALTZ-16," J. Mag. Reson. 53, 313-340 (1983).
- [4] Z. Starcuk, K. Bartusek, and Z. Starcuk, "Heteronuclear broadband spin-flip decoupling with adiabatic pulses," J. Mag. Reson. 107, 24-31 (1994).
- [5] E. Kupce and R. Freeman, "Adiabatic pulses for wideband inversion and broadband decoupling," J. Mag. Reson. 115, 273-276 (1995).
- [6] J. Cavanagh, W. J. Fairbrother, A. G. Palmer III, M. Rance, and N. J. Skelton, Protein NMR Spectroscopy: Principles and Practices (Elsevier Academic, 2007).

- [7] M. A. McCoy and L. Mueller, "Selective shaped pulse decoupling in NMR: Homonuclear [carbon-13]carbonyl decoupling," *J. Am. Chem. Soc.* 114, 2108-2112 (1992).
- [8] E. Kupce and G. Wagner, "Multisite band-selective decoupling in proteins," *J. Magn. Reson., Ser. B* 110, 309-312 (1996).
- [9] E. Kupce and G. Wagner, "Wideband homonuclear decoupling in protein spectra," *J. Magn. Reson., Ser. B* 109, 329-333 (1995).
- [10] J. Farjon, W. Bermel, and C. Griesinger, "Resolution enhancement in spectra of natural products dissolved in weakly orienting media with the help of ^1H homonuclear dipolar decoupling during acquisition: Application to ^1H - ^{13}C dipolar couplings measurements," *J. Mag. Reson.* 180, 72-82 (2006).
- [11] M. Goldman, *Quantum Description of High-Resolution NMR in Liquids* (Oxford University Press, 1988).
- [12] P. Owrutsky and N. Khaneja, "Control of inhomogeneous ensembles on the Bloch sphere," *Phys. Rev. A* 86, 022315 (2012).